Journal of proteome research

pubs.acs.org/jpr

Communication

Generation of SARS-CoV-2 S1 Spike Glycoprotein Putative Antigenic Epitopes in Vitro by Intracellular Aminopeptidases

George Stamatakis, Martina Samiotaki, Anastasia Mpakali, George Panayotou, and Efstratios Stratikos*

Cite This: https://dx.doi.org/10.1021/acs.jproteome.0c00457

Read Online

ACCESS | Metrics & More | Article Recommendations | Supporting Information

ABSTRACT: Presentation of antigenic peptides by MHCI is central to cellular immune responses against viral pathogens. While adaptive immune responses versus SARS-CoV-2 can be of critical importance to both recovery and vaccine efficacy, how protein antigens from this pathogen are processed to generate antigenic peptides is largely unknown. Here, we analyzed the proteolytic processing of overlapping precursor peptides spanning the entire sequence of the S1 spike glycoprotein of SARS-CoV-2, by three key enzymes that generate antigenic peptides, aminopeptidases ERAP1, ERAP2, and IRAP. All enzymes generated shorter peptides with sequences suitable for binding onto HLA alleles, but with distinct specificity fingerprints. ERAP1 was the most efficient in generating peptides 8−11 residues long, the optimal length for HLA binding, while IRAP was the least efficient. The combination of ERAP1 with ERAP2 greatly limited the variability of peptide sequences produced. Less than 7% of computationally predicted epitopes were found to be produced experimentally, suggesting that aminopeptidase processing may constitute a significant filter to epitope presentation. These experimentally generated putative epitopes could be prioritized for SARS-CoV-2 immunogenicity studies and vaccine design. We furthermore propose that this in vitro trimming approach could constitute a general filtering method to enhance the prediction robustness for viral antigenic epitopes.

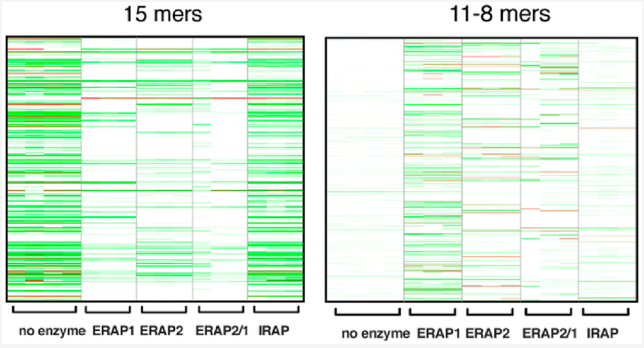

KEYWORDS: *enzyme, antigen, peptide, immune system, aminopeptidase, epitope, SARS-CoV-2, COVID-19, HLA, LC-MS/MS*

INTRODUCTION

Severe acute respiratory syndrome coronavirus 2 (SARS-CoV-2) is the pathogen responsible for coronavirus disease 19 (COVID-19) that is behind a major ongoing pandemic.[1−3] Virus entry into host cells is dependent on the S1 spike glycoprotein that forms homotrimers on the surface of the virion and interacts with the ACE2 receptor in susceptible cells.[4−6]

Many studies on clinical characteristics and mortality resulting from SARS-CoV-2 infection have highlighted the need for a detailed understanding of immune responses against this pathogen.[7] While appropriate innate and adaptive immune responses are necessary for recovery from infection, aberrant immune responses can be a major contributing factor to mortality.[8,9] In parallel, understanding immune recognition of SARS-CoV-2 is crucial to the ongoing massive global effort into developing an effecting vaccine against this pathogen.[10] Although early analyses have focused on the development of neutralizing antibodies, cellular immune responses are emerging of vital importance[11] both for understanding normal immune response against this pathogen and for designing and optimizing vaccines.[12] In particular, T-cell mediated immunity appears to be important for both viral clearance and for long-term immunity.[11] Thus, analysis of antigenic epitopes from SARS-CoV-2 should be a priority for the design of vaccines that induce effective and long-lasting cellular immune responses.[13]

Cytotoxic T-cell responses against virus-infected cells hinge on the presentation of small peptidic fragments of viral proteins, called antigenic peptides, by specialized proteins on the cell surface that belong to the Major Histocompatibility Class I complex (MHCI, also called Human Leukocyte Antigens, HLA, in humans). Antigenic peptides are derived from viral proteins that are proteolytically degraded by complex proteolytic cascades.[14] Intracellular aminopeptidases, ER aminopeptidase 1 (ERAP1), ER aminopeptidase 2 (ERAP2), and insulin-regulated aminopeptidase (IRAP) play important roles in producing antigenic peptides, by down-sizing longer peptides to the correct length for binding onto MHCI.[15] Appropriate processing of pathogen antigens by these enzymes can determine the generation of cytotoxic

Special Issue: Proteomics in Pandemic Disease

Received: June 23, 2020
Published: September 15, 2020

immune responses, and aberrant processing can lead to immune evasion.[16] Thus, it is important to understand how these enzymes process SARS-CoV-2 antigens, so as to gain insight into the efficacy of antiviral cytotoxic responses and reveal possible avenues to enhance them.

In this study, we utilized a novel approach to analyze antigen trimming by intracellular aminopeptidases ERAP1, ERAP2, and IRAP, focusing on the largest antigen of SARS-CoV-2, namely, S1 spike glycoprotein. By using tandem LC-MS/MS analysis, we were able to follow trimming in parallel of a large ensemble of peptides derived from the full length of S1 protein. This approach was inspired by two established observations: (i) that these enzymes are expected to normally encounter a very large number of potential substrates concurrently in the cell and (ii) accommodation of peptides inside a large cavity of each enzyme can lead to complex interactions between substrates that have to compete for the same space in the cavity.[17−19] Our analysis provides novel insight into the differences in substrate specificity between the three enzymes and provides a potential filter of traditional bioinformatic approaches that aim to predict antigenic epitopes. Finally, we propose a limited list of peptides that are potential ligands for common HLA alleles and could be prioritized for further immunological analyses and vaccine design efforts.

EXPERIMENTAL PROCEDURES

Enzyme Expression and Purification

Recombinant ERAP1, ERAP2, and IRAP were expressed and purified as described previously. Briefly, ERAP1 and ERAP2 were expressed by Hi5 insect cells in culture after infection with baculovirus carrying the appropriate gene and purified by affinity chromatography using a C-terminal his tag.[20,21] The enzymatic extracellular domain of IRAP was expressed by stably transfected HEK 293S GnTI$^{(-)}$ cells and purified by affinity chromatography using a C-terminal Rhodopsin 1D4 tag.[22] Enzymes were stored with 10% glycerol in aliquots at −80 °C until needed.

Peptides

The PepMix SARS-CoV-2 peptide mixture was purchased by JBT Peptide Technologies GmbH. Peptide pools were dissolved in DMSO. Prior to reactions the two peptide collections (158 and 157 peptides respectively) were mixed at equimolar concentrations and diluted in buffer containing 10 mM Hepes pH 7, 100 mM NaCl to a final concentration of 48 μM.

Enzymatic Reactions

Enzymatic reactions were performed in triplicate in a total volume of 50 μL in 10 mM Hepes pH 7, 100 mM NaCl. Freshly thawed enzyme stocks were added to each reaction to a final concentration of 50 nM. Reactions were incubated at 37 °C for 2 h, stopped by the addition of 7.5 μL of a 10% TFA solution, flash frozen in liquid nitrogen, and stored at −80 °C until analysis.

LC-MS/MS Analysis

The sample was preconcentrated on a pepmap LC trapping column (0.3 × 5 mm) at a rate of 30 μL of Buffer A (0.1% Formic acid in water) in 5 min. The LC gradient used was 5% Buffer B (0.1% Formic acid in Acetonitrile) to 25% in 36 min followed by an increase to 36% in 5 min and a second increase to 80% in 0.5 min and then was kept constant for 2 min. The column was equilibrated for 15 min prior to the next injection. A full MS was acquired with a Q Exactive HF-X Hybrid Quadropole-Orbitrap mass spectrometer, in the scan range of 350−1400 m/z using 60K resolving power with an AGC of 3×10^6 and max IT of 45 ms, followed by MS/MS scans of the 12 most abundant ions, using 15K resolving power with an AGC of 1×10^5 and max IT of 22 ms and an NCE of 28.

Database Search

We employed the MaxQuant computational proteomics platform version 1.6.14.0 to search the peak lists against the Spike glycoprotein SARS2 FASTA file (SwissProt accession number P0DTC2) and a file containing 247 frequently observed contaminants. N-terminal acetylation (42.010565 Da) and methionine oxidation (15.994915 Da) were set as variable modifications. The second peptide identification option in Andromeda was enabled. The false discovery rate (FDR) was set to 0.01 for both peptides. The enzyme specificity was set as unspecific. The minimum peptide length was set to 6 amino acids. The initial allowed mass deviation of the precursor ion was set to 4.5 ppm and the maximum fragment mass deviation was set to 20 ppm.

RESULTS AND DISCUSSION

To investigate the trimming of antigenic epitope precursors by intracellular aminopeptidases that generate antigenic peptides, we used a mixture of 315 synthetic peptides derived from the sequence of the SARS-CoV-2 S1 spike glycoprotein. All peptides were 15 residues long and spanned the entire sequence of the protein with an 11 residue overlap between adjacent peptides. This mixture allows the systematic sampling of the entire sequence of the protein. The peptide mixture was incubated with either ERAP1, ERAP2, or IRAP at a substrate to enzyme ratio of 1000:1 and the digestion products analyzed by LC-MS/MS using a custom search database generated by in silico digestions of the full S1 protein sequence (UniProt ID: P0DTC2). We also tested an equimolar mixture of ERAP1 and ERAP2 since previous studies have suggested that these two proteins can form functional equimolar heterodimers in cells.[23,24] All analyses were performed on three biological replicates for each reaction, as well as a control reaction that was performed in the absence of enzymes. An additional technical replicate for the control sample was also analyzed. For statistical robustness, we performed a t test between the control sample and each reaction and selected for further analysis only the peptides for which the quantification value changed by a statistically significant degree (p-value < 0.05).

The relative abundance of each peptide before and after the reaction was compared by label-free quantification. Analysis identified 263 unique 15mers in the samples out of the total 315 in the mixture. This represents an 83% coverage of included peptides which may be due to poor ionization and detection for some peptide sequences. As a result, further analysis was limited to the peptides detectable by our experimental setup. On average, incubation with the enzyme reduced the relative abundance of the 15mer peptides indicating successful digestion (Figure 1A,B). This reduction was much more evident for ERAP1 and ERAP2 (and their mixture) than for IRAP. Each enzyme featured a unique digestion fingerprint, suggesting different selectivity, as suggested in previous studies.[25] The full list of generated peptides is shown in Supplemental Table S1. Since the majority of peptides presented by HLA are 8−11 residues long, we analyzed the comparative abundance of 8−11mers

https://dx.doi.org/10.1021/acs.jproteome.0c00457
J. Proteome Res. XXXX, XXX, XXX−XXX

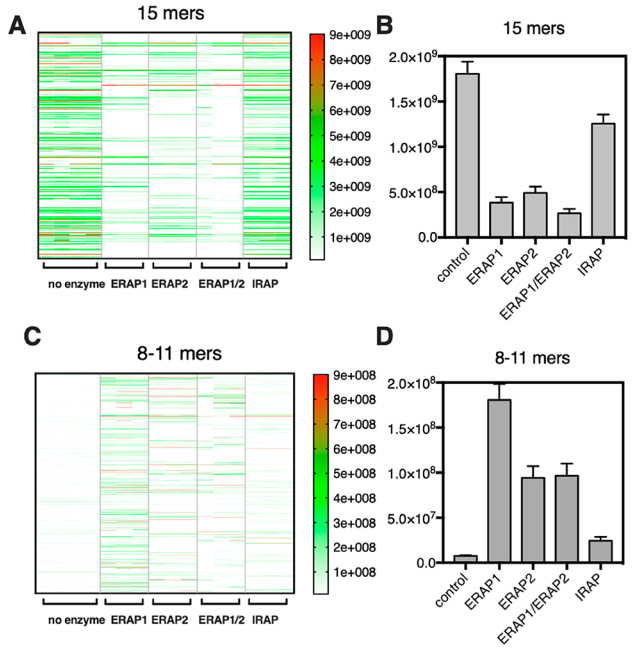

Figure 1. (A) Heatmap showing trimming of 15mers by aminopeptidases for each biological replicate. (B) Average label-free quantification (LFQ) signal of 15mers in the sample before and after incubation with the indicated enzyme. (C) Heatmap showing LFQ signal for 8−11mers produced after digestion. (D) Average signal of 8−11mers.

generated from each reaction (Figure 1C,D). Of the three enzymes, ERAP1 was the most efficient in generating peptides within this length range, consistent with previous reports on the mechanism of action of this enzyme.[17,26] ERAP2 and the ERAP1/ERAP2 mixture followed, while IRAP was the least efficient. Similar to the trimming of 15mers, the generation of 8−11mers followed a unique fingerprint for each enzyme. This is consistent with the previous hypotheses that each of these enzymes accommodate peptides in a large internal cavity and selectivity is driven by interactions with the whole sequence of the peptide.[17,21,22]

Indeed, comparing the peptide sequences generated by each enzyme, out of 1184 peptides identified, 142 were common between all three enzymes, 244 between ERAP1 and ERAP2 and 220 between ERAP1 and IRAP (Figure 2A). Furthermore, 169 peptides were unique for ERAP1, 234 for ERAP2, and 303 for IRAP. A similar situation was evident for 8−11mer peptides (Figure 2B). Strikingly, the mixture of ERAP1 with ERAP2 generated the fewest number of distinct sequences of 8−11mers (Figure 2C). This was in contrast to the finding that the ERAP1/ERAP2 mixture generated about the same average signal intensity as ERAP2 (Figure 1D). This was due to ERAP1/ERAP2 mixture generating fewer, in terms of sequence, distinct peptides, which were however relatively abundant. This finding is consistent with the proposed synergism of ERAP1 and ERAP2[27] and suggests that the combination of these two enzymes is more efficient in trimming variable sequences and can thus overtrim peptides to lengths below 7 residues that are not detectable in our experimental setup and should not be able to stably bind onto MHCI (Figure 2C). As a result, incubation with ERAP1/ERAP2 mixture accumulates only peptides that are resistant to degradation by both enzymes.

Since epitope length is a key parameter for binding onto MHCI (the majority of presented peptides are 9mers) we analyzed the distribution of lengths of peptides generated by each enzymatic reaction (Figure 3). ERAP1 was very efficient in trimming the 15mer substrates and generated primarily 9mer peptides, consistent with its proposed property as a "molecular ruler".[26] Neither ERAP2 nor IRAP were able to accumulate 9mers preferably, but still generated significant numbers. The mixture of ERAP1 and ERAP2 showed a similar fractional distribution of peptide lengths (Figure 3B), but produced a much lower number of distinct peptide sequences (Figure 3A), presumably due to overtrimming to smaller lengths or even single amino acids.

The main determinant in antigen presentation is stable binding of antigen-generated peptides onto MHCI. To evaluate the potential of the generated peptides to bind onto MHCI we used the HLAthena prediction server to rank the peptides for binding onto a collection of common HLA alleles[29] specifically HLA-A01:01, HLA-A02:01, HLA-A03:01, HLA-A24:02, HLA-A26:01, HLA-B07:02, HLA-B08:01, HLA-B27:05, HLA-B39:01, HLA-B40:01, HLA-B58:01, and HLA-B15:01 (Supplemental Table S2). For each peptide we selected the best scoring HLA-allele and plotted the calculated percentile rank of the predicted score for each enzymatic reaction (Figure 4A). The geometric mean of the predicted affinity was lowest for ERAP1 (indicating that the ERAP1 generated peptides had the highest average affinity for HLA),

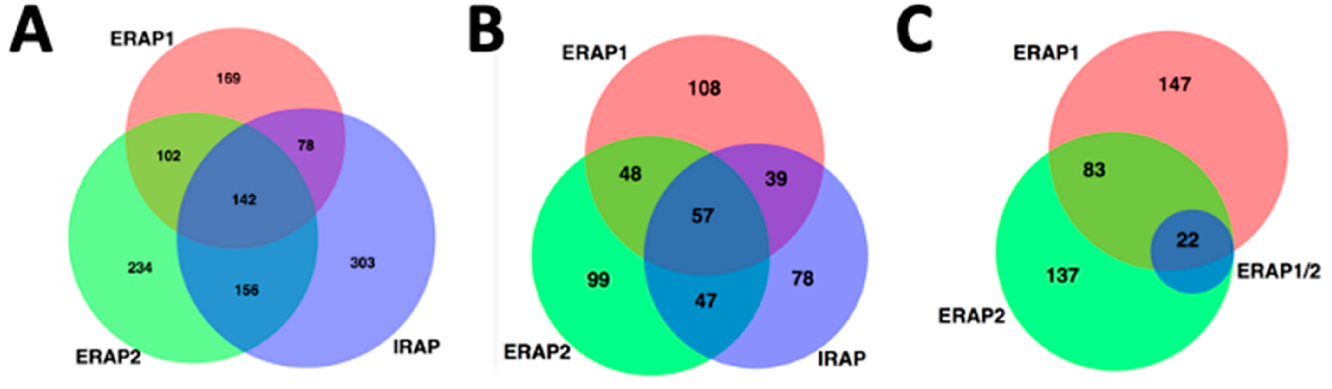

Figure 2. Venn diagrams indicating overlap between peptide sequences produced by each enzyme. Numerals indicate number of peptides in each segment. Analysis was performed using BioVenn.[28] (A) Comparison of all peptides produced by each enzyme. (B) Comparison of 8−11mers produced by each enzyme. (C) Comparison of 8−11mers produced by ERAP1, ERAP2, as well as their mixture (ERAP1/2).

https://dx.doi.org/10.1021/acs.jproteome.0c00457
J. Proteome Res. XXXX, XXX, XXX−XXX

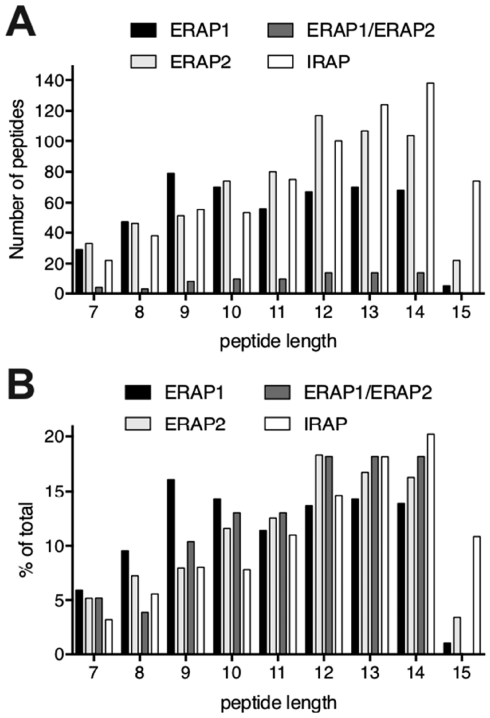

Figure 3. Length distribution of peptides detected by LC-MS/MS after enzymatic digestion. (A) Number of peptides detected of each length. (B) Relative fraction of each length compared to the total number of peptides detected.

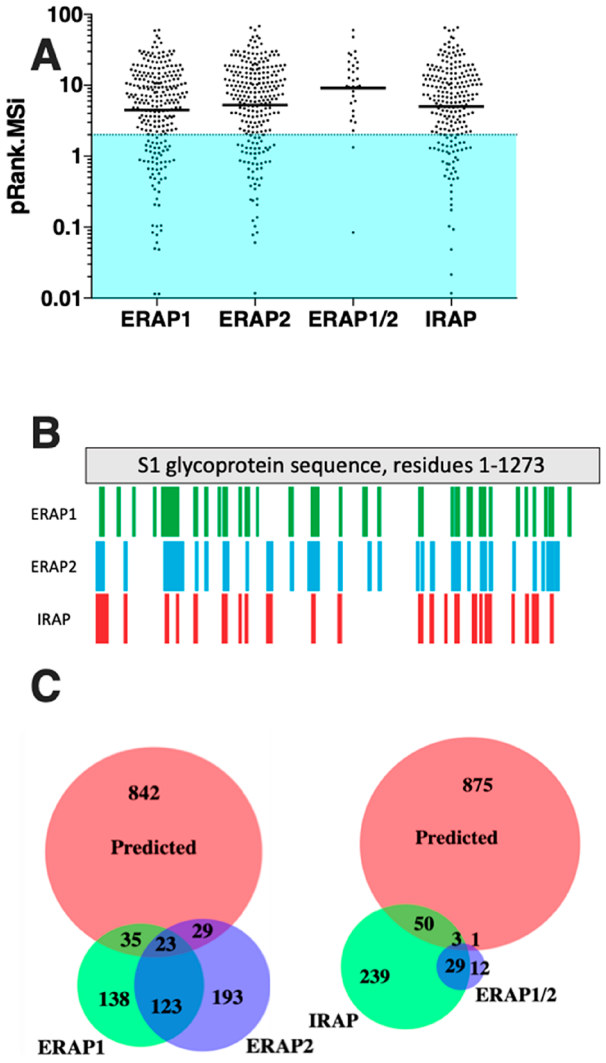

Figure 4. (A) Scatter plot showing the predicted affinity of produced peptides for common HLA alleles as calculated by HLAthena. Color region encompasses peptides that are predicted to bind to at least one of the common HLA alleles used in the analysis. (B) Schematic representation of relative locations in the S1 protein sequence where the generated peptides are found. (C) Venn diagrams depicting overlap between peptides of S1 protein predicted to bind to common HLA alleles and peptides produced experimentally by ERAP1, ERAP2, IRAP, or ERAP1/ERAP2 mixture. Numerals indicate number of peptides in each separate segment.

followed by IRAP and then ERAP2. Only a subset of generated peptides was predicted to bind with sufficient affinity onto at least one HLA: 23% for ERAP1, 22% for ERAP2, 6% for ERAP1/ERAP2 mixture, and 21% for IRAP (peptide sequences are listed in Table 1). These peptides spanned the whole sequence of the S1 spike glycoprotein, although each enzyme presented a unique signature onto this sequence (Figure 4B). Although currently we cannot know if any of these peptides can be antigenic, we compared them to known antigenic peptides for SARS-CoV-1 found in the immune epitope database (http://www.iedb.org/).[30] ERAP1 generated 5 antigenic peptides reported to be antigenic for SARS-CoV-1, ERAP2 generated 4, and IRAP 1. This finding indicates that some cross-reactivity between SARS-CoV-1 and SARS-CoV-2 may be mediated through the generation of appropriate epitopes by intracellular aminopeptidases.

In a recent publication, the authors proposed that different HLA alleles can have significant variability in their ability to present SARS-CoV-2 epitopes, with HLA-B46:01 having the capability to present the fewest and HLA-B15:03 being able to present the most.[31] We thus used the NetMHCpan 4.1 server to predict potential epitopes form the S1 spike glycoprotein sequence that could be presented by HLA-B46:01 and HLA-B15:03 (Supplemental Table S3) and compared them to the experimentally produced peptides. ERAP1 was found to produce 15 potential ligands for HLA-B15:03 but only 6 for HLA-B46:01, consistent with the proposed trend. In contrast, ERAP2 produced 8 potential ligands for both alleles and IRAP produced 6 for HLA-B15:03 and 4 for HLA-B46:01. Strikingly, the mixture of ERAP1 with ERAP2 produced 3 peptides that could bind onto HLA-B15:03, but no peptides predicted to bind onto HLA-B46:01 (Table 2). Thus, our findings appear to validate the hypothesis that HLA-B15:03 is likely to present more SARS-CoV-2 epitopes than HLA-B46:01, but only for ERAP1, which however is considered the dominant amino-peptidase activity in the cell for generating antigenic peptides.

Bioinformatic epitope predictions based on antigen sequence are often used as a tool to study the potential antigenicity of a particular epitope or pathogen. The power of those predictions is constantly evolving and primarily relies on predictions of binding affinity on HLA. To compare such predictions to our experimentally generated peptides, we used the full sequence of the S1 spike glycoprotein and the NetMHCpan 4.1 server[32] to predict potential epitopes that could be presented by the common HLA alleles indicated in the previous paragraph. The server predicted 929 potential epitopes with lengths of 8−12 residues (Supplemental Table S4). Of those potential epitopes, however, less than 7% were found to be produced experimentally by one of the enzymes

https://dx.doi.org/10.1021/acs.jproteome.0c00457
J. Proteome Res. XXXX, XXX, XXX−XXX

Table 1. Peptides Generated by Each Aminopeptidase and Are Predicted to Bind onto at Least One of the Common HLA-Alleles[a]

ERAP1			ERAP2			IRAP		
peptide	score	allele	peptide	score	allele	peptide	score	allele
KFLPFQQF	0.01	A2402	EVFNATRF	0.00	A2601	EVFNATRF	0.00	A2601
VYYPDKVF	0.01	A2402	VLNDILSR	0.01	A0301	VLNDILSR	0.01	A0301
GYLQPRTF	0.05	A2402	GRLQSLQTY	0.06	B2705	HADQLTPTW	0.02	B5801
VRFPNITNL	0.05	B2705	YRFNGIGV	0.08	B2705	GYLQPRTF	0.05	A2402
GRLQSLQTY	0.06	B2705	**NQKLIANQF**	0.08	B1501	LADAGFIKQY	0.09	A0101
YRFNGIGV	0.08	B2705	DAGFIKQY	0.10	A2601	DAGFIKQY	0.10	A2601
NQKLIANQF	0.08	B1501	SLGAENSVAY	0.12	B1501	NYNYLYRL	0.18	A2402
NLREFVFK	0.09	A0301	VFKNIDGYFKI	0.14	A2402	STEKSNIIRGW	0.21	B5801
DAGFIKQY	0.10	A2601	STEKSNIIRGW	0.21	B5801	TLADAGFIK	0.25	A0301
DSFKEELDKY	0.10	A2601	ILSRLDKV	0.24	A0201	GVYYPDKVF	0.32	B1501
SVASQSIIAY	0.11	B1501	FKEELDKY	0.24	A0101	TLADAGFIKQY	0.39	A2601
TYVPAQEKNF	0.20	A2402	TRFASVYAWNR	0.25	B2705	ALNTLVKQL	0.48	A0201
KRFDNPVLPFN	0.21	B2705	QRNFYEPQI	0.35	B2705	KVTLADAGFIK	0.48	A0301
TLADAGFIK	0.25	A0301	IEDLLFNK	0.38	A0101	YADSFVIR	0.49	A0101
GVYYPDKVF	0.32	B1501	LPIGINITRF	0.39	B0702	PFGEVFNATRF	0.52	A2402
ATRFASVY	0.34	A0101	LGAENSVAY	0.41	B1501	GAGAALQI	0.57	B5801
GVYYPDKV	0.39	A0201	**LPQGFSAL**	0.47	B0702	APHGVVFL	0.61	B0702
SVLNDILSR	0.42	A0301	TRFQTLLA	0.49	B2705	NIDGYFKI	0.65	A0101
LPQGFSAL	0.47	B0702	YADSFVIR	0.49	A0101	ITGRLQSLQTY	0.68	A0101
KVTLADAGFIK	0.48	A0301	**TPINLVRDL**	0.50	B0702	TRGVYYPDKVF	0.78	B2705
YADSFVIR	0.49	A0101	APHGVVFL	0.61	B0702	QLTPTWRV	0.79	A0201
TPINLVRDL	0.50	B0702	DPLSETKCTL	0.66	B0702	YPDKVFRSSV	0.83	B0702
NYKLPDDF	0.56	A2402	ALGKLQDV	0.66	A0201	VLYENQKLI	0.84	A0201
NFYEPQII	0.57	A2402	ITGRLQSLQTY	0.68	A0101	NTLVKQLSSNF	0.89	A2601
NIDGYFKI	0.65	A0101	TRGVYYPDKVF	0.78	B2705	TTDNTFVS	0.96	A0101
DPLSETKCTL	0.66	B0702	QLTPTWRV	0.79	A0201	**LPPAYTNSF**	1.10	B0702
ALGKLQDV	0.66	A0201	GINITRFQTL	0.79	B0801	QRNFYEPQII	1.15	B2705
NESLIDLQEL	0.67	B4001	QPYRVVVLSF	0.82	B0702	QPRTFLLKY	1.16	A0101
FVIRGDEV	0.71	A0201	LYENQKLI	0.83	A2402	NVYADSFVIR	1.19	A0301
QLTPTWRV	0.79	A0201	YPDKVFRSSV	0.83	B0702	GEVFNATRF	1.21	B4001
QPYRVVVLSF	0.82	B0702	VLYENQKLI	0.84	A0201	EELDKYFKNH	1.24	A2601
LYENQKLI	0.83	A2402	GVLTESNKKF	0.87	A2601	YYPDKVFRSSV	1.24	A2402
YPDKVFRSSV	0.83	B0702	VRDLPQGFSAL	0.93	B2705	AEVQIDRLITG	1.29	B4001
KNIDGYFKI	0.84	A2402	DPLQPELDSF	1.09	B0702	EPLVDLPI	1.30	B0702
VLYENQKLI	0.84	A0201	**LPPAYTNSF**	1.10	B0702	TGRLQSLQTY	1.31	B1501
VYADSFVIR	0.85	A2402	DILSRLDKV	1.11	B0801	SVLHSTQDLFL	1.33	A0201
TVYDPLQP	0.88	A0301	NGIGVTQNVLY	1.12	A2601	YGVSPTKL	1.37	A2601
HFPREGVF	0.89	A2402	QRNFYEPQII	1.15	B2705	VTLADAGFIK	1.39	A0301
QDVVNQNAQAL	0.93	B4001	QPRTFLLKY	1.16	A0101	LPFQQFGRDIA	1.44	B0801
FEYVSQPF	0.96	B4001	EELDKYFKNH	1.24	A2601	QKFNGLTVLPP	1.45	B2705
SIIAYTMSL	1.04	B0801	LPFQQFGRDI	1.29	B0702	DGYFKIYSKH	1.55	A2601
KKFLPFQQFGR	1.11	B2705	EPLVDLPI	1.30	B0702	YENQKLIANQF	1.55	B1501
DILSRLDKV	1.11	B0801	TGRLQSLQTY	1.31	B1501	FPREGVFVSN	1.56	B0702
QPRTFLLKY	1.16	A0101	QKLIANQF	1.31	B1501	GNYNYLYRL	1.63	B2705
NVYADSFVIR	1.19	A0301	TTEILPVSM	1.32	A0101	NATRFASVY	1.82	A2601
GEVFNATRF	1.21	B4001	SPDVDLGDISG	1.33	B0702	YRLFRKSNLKP	1.83	B2705
EELDKYFKNH	1.24	A2601	DVVIGIVNN	1.42	A2601	HADQLTPTWRV	1.98	A0101
QKLIANQF	1.31	B1501	LPFQQFGRDIA	1.44	B0801	YVTQQLIRA	2.00	A0201
TTEILPVSM	1.32	A0101	QKFNGLTVLPP	1.45	B2705			
SLLIVNNA	1.37	A0201	DIADTTDAVRD	1.52	A2601			
YGVSPTKL	1.37	A2601	DGYFKIYSKH	1.55	A2601			
VTLADAGFIK	1.39	A0301	GNYNYLYRL	1.63	B2705			
VGYQPYRV	1.42	A0201	SRLDKVEAEV	1.64	B2705			
DIADTTDAVRD	1.52	A2601	NATRFASVY	1.82	A2601			
DGYFKIYSKH	1.55	A2601	YRLFRKSNLKP	1.83	B2705			
RDLPQGFSAL	1.55	B4001	HADQLTPTWRV	1.98	A0101			
LEPLVDLPI	1.64	B4001	YVTQQLIRA	2.00	A0201			
SRLDKVEAEV	1.64	B2705						

https://dx.doi.org/10.1021/acs.jproteome.0c00457
J. Proteome Res. XXXX, XXX, XXX−XXX

Table 1. continued

ERAP1			ERAP2			IRAP		
peptide	score	allele	peptide	score	allele	peptide	score	allele
NATRFASVY	1.82	A2601						
YVTQQLIRA	2.00	A0201						

[a]HLA-A01:01, HLA-A02:01, HLA-A03:01, HLA-A24:02, HLA-A26:01, HLA-B07:02, HLA-B08:01, HLA-B27:05, HLA-B39:01, HLA-B40:01, HLA-B58:01, and HLA-B15:01. Scores indicated are percentile ranks corresponding to the predicted affinity score for each allele (range 0−100, 0 is best, ranks below 2 are considered binders). In bold are peptides reported to be antigenic for SARS-CoV-1 found in the immune epitope database (http://www.iedb.org/).

Table 2. Peptides Generated by Each Aminopeptidase That Are Predicted to Bind to HLA-B15:03 and HLA-B46:01[a]

ERAP1		ERAP2		IRAP		ERAP1/ERAP2	
sequence	score	sequence	score	sequence	score	sequence	score
HLA-B15:03		**HLA-B15:03**		**HLA-B15:03**		**HLA-B15:03**	
ATRFASVY	0.37	VGYLQPRTF	0.53	VGYLQPRTF	0.53	VGYLQPRTF	0.54
VGYLQPRTF	0.53	NQKLIANQF	0.58	LKYNENGTITD	1.40	NQKLIANQF	0.58
NQKLIANQF	0.58	GRLQSLQTY	0.65	GYLQPRTF	1.59	LKYNENGTITD	1.41
GRLQSLQTY	0.65	LGAENSVAY	0.84	GEVFNATRF	1.63		
FEYVSQPF	0.83	QKLIANQF	0.91	GVYYPDKVF	1.71		
QKLIANQF	0.91	LKYNENGTITD	1.40	AGAALQIPF	1.91		
KAHFPREGVF	1.34	SLGAENSVAY	1.48				
LKYNENGTITD	1.40	NGIGVTQNVLY	1.89				
AQYTSALLA	1.42						
KRFDNPVLPFN	1.58						
GYLQPRTF	1.59						
SVASQSIIAY	1.59						
GEVFNATRF	1.63						
GVYYPDKVF	1.71						
VYYPDKVF	1.80						
HLA-B46:01		**HLA-B46:01**		**HLA-B46:01**		**HLA-B46:01**	
FEYVSQPF	0.62	LGAENSVAY	0.037	TLADAGFIKQY	0.08	–	
SIIAYTMSL	0.64	LPIGINITRF	0.71	YVGYLQPRTF	1.66		
ATRFASVY	0.65	SLGAENSVAY	0.72	GVYYPDKVF	1.75		
SVASQSIIAY	0.91	GVLTESNKKF	1.34	TGRLQSLQTY	1.98		
IANQFNSAI	1.25	YVGYLQPRTF	1.65				
GVYYPDKVF	1.75	NGIGVTQNVLY	1.84				
		FKEELDKY	1.90				
		TGRLQSLQTY	1.98				

[a]Scores indicated are percentile ranks corresponding to the predicted score for each allele (range 0−100, 0 is best, ranks below 2 are considered binders).

tested and more specifically 58 by ERAP1, 52 by ERAP2, 4 for the ERAP1/2 mixture, and 53 by IRAP (Figure 4C). This finding suggests that intracellular antigen processing by aminopeptidases can significantly limit which peptides can be presented by MHCI. Indeed, it has been recently proposed that the main function of ERAP1 is to limit the peptide pool available for MHCI.[33] In this context, this experimental approach could be useful in optimizing bioinformatic predictions of potential MHCI epitopes.

Our findings provide new information on both the general biological functions of intracellular aminopeptidases that generate antigenic peptides as well as on specific processing of a key antigen from SARS-CoV-2. Specifically, our results highlight that each enzyme bears a unique trimming fingerprint to antigen processing. Although this has been suggested before on the basis of differences in specificity toward specific peptide substrates,[23,27,34,35] it has not been observed in the context of peptide ensembles. This is potentially important since competition of different peptides for the cavity in these enzymes could result in complex substrate interactions. At first glance, major differences in trimming fingerprints between each or the three enzymes, may appear to impose an unnecessary complication to antigenic peptide generation. It is conceivable, however, that this trimming variability is desirable for the immune system, since it can expand the breadth of possible antigenic peptides detected in different immunological settings and cell types. Our results also highlight a previously proposed property of ERAP1: the specialization in trimming large peptides and producing peptides that have the ideal length for MHCI binding—most of the ERAP1 products fall well within that range.[26] In contrast, both ERAP2 and IRAP appear to be less optimized for length selection. However, they are still able to produce many peptides that are potential cargo for MHCI, casting some doubt on whether the unique trimming properties of ERAP1 are absolutely necessary for this basic function. Furthermore, the combination of ERAP1 with ERAP2 appears to provide significant synergism in trimming, to the point of overtrimming peptides and limiting available sequences. Synergism between ERAP1 and ERAP2 has been demonstrated before in trimming

https://dx.doi.org/10.1021/acs.jproteome.0c00457
J. Proteome Res. XXXX, XXX, XXX−XXX

isolated peptides and these two enzymes have been proposed to also form functional dimers.[23,24] According to our observations, their combination is especially efficient in trimming. While the biological repercussions of this are not fully clear yet, it is conceivable that the strong associations between ERAP2 activity and predisposition to autoimmunity may be related to this effect.[36]

Despite the current importance in understanding immune reactions in COVID-19, very little is known about the cellular adaptive immune responses against SARS-CoV-2. Cellular immune responses are emerging as a central player in clearing the infection and as targets for vaccine efforts.[37,38] Furthermore, HLA polymorphic variation has been suggested to underlie the large variability in virus clearance that has been observed among individuals.[39] Our analysis of the largest antigen of SARS-CoV-2, S1 spike glycoprotein, suggests that aminopeptidase trimming can be a significant filter that helps shape which peptides will be presented by HLA. Thus, we propose a short list of candidate peptides that could be prioritized in downstream antigenic analysis as well as in vaccine design and efficacy studies (Tables 1 and 2).

While the functions of ERAP1, ERAP2, and IRAP have been studied in both in vitro and in vivo contexts during the past decade, their relative functional differences have only been compared in processing specific substrates at a time. However, all these enzymes have a broad substrate specificity and can normally encounter thousands of different peptides in the ER or endosomal compartments. On the other hand, studies focusing on the presented immunopeptidome have revealed effects attributed to ERAP1 and ERAP2 trimming, but direct comparisons have been difficult because of the dominant effect of MHCI affinity on presentation.[40] Our approach stands in-between these two types of studies. It mimics the multiple-substrate situation that is likely normal in vivo but focuses on antigenic peptide precursor trimming. In this context, our approach may have broader application for the quick prediction of potential antigenic epitopes as an additional filter on bioinformatic predictions. Indeed, bioinformatic predictions result in many candidate peptides, very few of which will provoke an immune response; adding more filters can increase the usefulness of these rapid approaches. However, our approach also has limitations that need to be taken into account when interpreting results. Due to differences in ionization and detection by the LC-MS/MS some peptides may not be detected or may be under-represented compared to other sequences, making comparisons between different peptides less reliable. Furthermore, it is an in vitro approach that is limited to the peptide pool used and cannot take into account the dynamics of MHCI binding that can protect peptides from further aminopeptidase degradation[41] or peptide proofreading by chaperone components or the peptide loading complex.[42] Due to those limitations, we restricted our analysis to statistical comparisons and avoided drawing conclusions regarding particular peptide sequences. Recent studies have also suggested that ERAP1 may trim peptides while they are bound onto MHCI.[43] Further systematic analysis of this phenomenon however, suggested that it is either very rare or misinterpreted in the case of rapid-dissociating peptides.[44] We therefore did not attempt to characterize trimming of prebound peptides in this study.

In summary, we analyzed the trimming of a peptide ensemble spanning the sequence of the S1 spike glycoprotein of SARS-CoV-2, the pathogen responsible for the recent COVID-19 pandemic. Our analysis provided novel insight into the function of antigen trimming enzymes and suggested that aminopeptidase trimming may be a significant filter in determining which peptides can be presented by MHCI. Furthermore, we have identified a limited set of peptides that were experimentally produced by elongated precursors which could be prioritized in future studies aiming to investigate the antigenicity of SARS-CoV-2 infected cells and assist in the design of highly effective vaccines that aim to produce adaptive cytotoxic responses. We propose that our experimental approach may also be useful as a general tool for enhancing bioinformatic predictions of antigenic epitopes.

■ ASSOCIATED CONTENT

Supporting Information

The Supporting Information is available free of charge at https://pubs.acs.org/doi/10.1021/acs.jproteome.0c00457.

Table S1: List of generated peptides after digestion by each enzyme (XLSX)

Table S2: List of generated 8−11mers from each enzyme with best predicted binding score based on the HLAthena server (XLSX)

Table S3: Predicted binding score of peptides from the S1 spike glycoprotein of SARS-CoV-2 for HLA-B15:03 and HLA-B46:01, based on the HLAthena prediction server; in red, the peptides that are predicted to be binders (XLSX)

Table S4: List of potential epitopes from the sequence of the S1 spike glycoprotein of SARS-CoV-2 predicted using the NetMHCpan 4.1 server (XLSX)

■ AUTHOR INFORMATION

Corresponding Author

Efstratios Stratikos − *National Centre for Scientific Research "Demokritos", 15310 Agia Paraskevi, Attica, Greece;* orcid.org/0000-0002-3566-2309; Email: stratos@rrp.demokritos.gr, stratikos@gmail.com

Authors

George Stamatakis − *Biomedical Sciences Research Center "Alexander Fleming", 16672 Vari, Attica, Greece*

Martina Samiotaki − *Biomedical Sciences Research Center "Alexander Fleming", 16672 Vari, Attica, Greece*

Anastasia Mpakali − *National Centre for Scientific Research "Demokritos", 15310 Agia Paraskevi, Attica, Greece;* orcid.org/0000-0003-0869-9680

George Panayotou − *Biomedical Sciences Research Center "Alexander Fleming", 16672 Vari, Attica, Greece*

Complete contact information is available at: https://pubs.acs.org/10.1021/acs.jproteome.0c00457

Funding

This research was supported by NCSR Demokritos and by "InfrafrontierGR/Phenotypos" (MIS 5002135) and by "The Greek Research Infrastructure for Personalised Medicine (pMED-GR)" (MIS 5002802), both funded by the Operational Programme "Competitiveness, Entrepreneurship and Innovation" (NSRF 2014−2020) and cofinanced by Greece and the EU (ERDF).

Notes

The authors declare no competing financial interest.

https://dx.doi.org/10.1021/acs.jproteome.0c00457
J. Proteome Res. XXXX, XXX, XXX−XXX

The mass spectrometry proteomics data have been deposited to the ProteomeXchange Consortium via the PRIDE[45] partner repository with the data set identifier PXD019901 (http://www.ebi.ac.uk/pride/archive/).

REFERENCES

(1) Coronaviridae Study Group of the International Committee on Taxonomy of Viruses. The species Severe acute respiratory syndrome-related coronavirus: classifying 2019-nCoV and naming it SARS-CoV-2. *Nat. Microbiol.* **2020**, *5* (4), 536−544.

(2) Wu, F.; Zhao, S.; Yu, B.; Chen, Y. M.; Wang, W.; Song, Z. G.; Hu, Y.; Tao, Z. W.; Tian, J. H.; Pei, Y. Y.; Yuan, M. L.; Zhang, Y. L.; Dai, F. H.; Liu, Y.; Wang, Q. M.; Zheng, J. J.; Xu, L.; Holmes, E. C.; Zhang, Y. Z. A new coronavirus associated with human respiratory disease in China. *Nature* **2020**, *579* (7798), 265−269.

(3) Zhou, P.; Yang, X. L.; Wang, X. G.; Hu, B.; Zhang, L.; Zhang, W.; Si, H. R.; Zhu, Y.; Li, B.; Huang, C. L.; Chen, H. D.; Chen, J.; Luo, Y.; Guo, H.; Jiang, R. D.; Liu, M. Q.; Chen, Y.; Shen, X. R.; Wang, X.; Zheng, X. S.; Zhao, K.; Chen, Q. J.; Deng, F.; Liu, L. L.; Yan, B.; Zhan, F. X.; Wang, Y. Y.; Xiao, G. F.; Shi, Z. L. A pneumonia outbreak associated with a new coronavirus of probable bat origin. *Nature* **2020**, *579* (7798), 270−273.

(4) Tortorici, M. A.; Veesler, D. Structural insights into coronavirus entry. *Adv. Virus Res.* **2019**, *105*, 93−116.

(5) Walls, A. C.; Park, Y. J.; Tortorici, M. A.; Wall, A.; McGuire, A. T.; Veesler, D. Structure, Function, and Antigenicity of the SARS-CoV-2 Spike Glycoprotein. *Cell* **2020**, *181* (2), 281−292.

(6) Shang, J.; Ye, G.; Shi, K.; Wan, Y.; Luo, C.; Aihara, H.; Geng, Q.; Auerbach, A.; Li, F. Structural basis of receptor recognition by SARS-CoV-2. *Nature* **2020**, *581* (7807), 221−224.

(7) St John, A. L.; Rathore, A. P. S. Early Insights into Immune Responses during COVID-19. *J. Immunol.* **2020**, *205* (3), 555−564.

(8) Song, P.; Li, W.; Xie, J.; Hou, Y.; You, C. Cytokine storm induced by SARS-CoV-2. *Clin. Chim. Acta* **2020**, *509*, 280−287.

(9) Li, K.; Hao, Z.; Zhao, X.; Du, J.; Zhou, Y. SARS-CoV-2 infection-induced immune responses: Friends or foes? *Scand. J. Immunol.* **2020**, *92* (2), No. e12895.

(10) Peeples, L. News Feature: Avoiding pitfalls in the pursuit of a COVID-19 vaccine. *Proc. Natl. Acad. Sci. U. S. A.* **2020**, *117* (15), 8218−8221.

(11) Leslie, M. T cells found in coronavirus patients 'bode well' for long-term immunity. *Science* **2020**, *368* (6493), 809−810.

(12) Manners, C.; Larios Bautista, E.; Sidoti, H.; Lopez, O. J. Protective Adaptive Immunity Against Severe Acute Respiratory Syndrome Coronaviruses 2 (SARS-CoV-2) and Implications for Vaccines. *Cureus* **2020**, *12* (6), No. e8399.

(13) Mukherjee, S.; Tworowski, D.; Detroja, R.; Mukherjee, S. B.; Frenkel-Morgenstern, M. Immunoinformatics and Structural Analysis for Identification of Immunodominant Epitopes in SARS-CoV-2 as Potential Vaccine Targets. *Vaccines (Basel, Switz.)* **2020**, *8* (2), 290.

(14) Rock, K. L.; Goldberg, A. L. Degradation of cell proteins and the generation of MHC class I-presented peptides. *Annu. Rev. Immunol.* **1999**, *17*, 739−79.

(15) Weimershaus, M.; Evnouchidou, I.; Saveanu, L.; van Endert, P. Peptidases trimming MHC class I ligands. *Curr. Opin. Immunol.* **2013**, *25* (1), 90−6.

(16) Hammer, G. E.; Kanaseki, T.; Shastri, N. The final touches make perfect the peptide-MHC class I repertoire. *Immunity* **2007**, *26* (4), 397−406.

(17) Giastas, P.; Mpakali, A.; Papakyriakou, A.; Lelis, A.; Kokkala, P.; Neu, M.; Rowland, P.; Liddle, J.; Georgiadis, D.; Stratikos, E. Mechanism for antigenic peptide selection by endoplasmic reticulum aminopeptidase 1. *Proc. Natl. Acad. Sci. U. S. A.* **2019**, *116* (52), 26709−26716.

(18) Stratikos, E.; Stern, L. J. Antigenic peptide trimming by ER aminopeptidases–insights from structural studies. *Mol. Immunol.* **2013**, *55* (3−4), 212−9.

(19) Evnouchidou, I.; Kamal, R. P.; Seregin, S. S.; Goto, Y.; Tsujimoto, M.; Hattori, A.; Voulgari, P. V.; Drosos, A. A.; Amalfitano, A.; York, I. A.; Stratikos, E. Coding single nucleotide polymorphisms of endoplasmic reticulum aminopeptidase 1 can affect antigenic peptide generation in vitro by influencing basic enzymatic properties of the enzyme. *J. Immunol.* **2011**, *186* (4), 1909−13.

(20) Stamogiannos, A.; Maben, Z.; Papakyriakou, A.; Mpakali, A.; Kokkala, P.; Georgiadis, D.; Stern, L. J.; Stratikos, E. Critical Role of Interdomain Interactions in the Conformational Change and Catalytic Mechanism of Endoplasmic Reticulum Aminopeptidase 1. *Biochemistry* **2017**, *56* (10), 1546−1558.

(21) Mpakali, A.; Giastas, P.; Mathioudakis, N.; Mavridis, I. M.; Saridakis, E.; Stratikos, E. Structural Basis for Antigenic Peptide Recognition and Processing by Endoplasmic Reticulum (ER) Aminopeptidase 2. *J. Biol. Chem.* **2015**, *290* (43), 26021−32.

(22) Mpakali, A.; Saridakis, E.; Harlos, K.; Zhao, Y.; Papakyriakou, A.; Kokkala, P.; Georgiadis, D.; Stratikos, E. Crystal Structure of Insulin-Regulated Aminopeptidase with Bound Substrate Analogue Provides Insight on Antigenic Epitope Precursor Recognition and Processing. *J. Immunol.* **2015**, *195* (6), 2842−2851.

(23) Saveanu, L.; Carroll, O.; Lindo, V.; Del Val, M.; Lopez, D.; Lepelletier, Y.; Greer, F.; Schomburg, L.; Fruci, D.; Niedermann, G.; van Endert, P. M. Concerted peptide trimming by human ERAP1 and ERAP2 aminopeptidase complexes in the endoplasmic reticulum. *Nat. Immunol.* **2005**, *6* (7), 689−97.

(24) Evnouchidou, I.; Weimershaus, M.; Saveanu, L.; van Endert, P. ERAP1-ERAP2 dimerization increases peptide-trimming efficiency. *J. Immunol.* **2014**, *193* (2), 901−8.

(25) Zervoudi, E.; Papakyriakou, A.; Georgiadou, D.; Evnouchidou, I.; Gajda, A.; Poreba, M.; Salvesen, G. S.; Drag, M.; Hattori, A.; Swevers, L.; Vourloumis, D.; Stratikos, E. Probing the S1 specificity pocket of the aminopeptidases that generate antigenic peptides. *Biochem. J.* **2011**, *435* (2), 411−20.

(26) Chang, S. C.; Momburg, F.; Bhutani, N.; Goldberg, A. L. The ER aminopeptidase, ERAP1, trims precursors to lengths of MHC class I peptides by a "molecular ruler" mechanism. *Proc. Natl. Acad. Sci. U. S. A.* **2005**, *102* (47), 17107−12.

(27) Lorente, E.; Barriga, A.; Johnstone, C.; Mir, C.; Jimenez, M.; Lopez, D. Concerted in vitro trimming of viral HLA-B27-restricted ligands by human ERAP1 and ERAP2 aminopeptidases. *PLoS One* **2013**, *8* (11), No. e79596.

(28) Hulsen, T.; de Vlieg, J.; Alkema, W. BioVenn - a web application for the comparison and visualization of biological lists using area-proportional Venn diagrams. *BMC Genomics* **2008**, *9*, 488.

(29) Sarkizova, S.; Klaeger, S.; Le, P. M.; Li, L. W.; Oliveira, G.; Keshishian, H.; Hartigan, C. R.; Zhang, W.; Braun, D. A.; Ligon, K. L.; Bachireddy, P.; Zervantonakis, I. K.; Rosenbluth, J. M.; Ouspenskaia, T.; Law, T.; Justesen, S.; Stevens, J.; Lane, W. J.; Eisenhaure, T.; Lan Zhang, G.; Clauser, K. R.; Hacohen, N.; Carr, S. A.; Wu, C. J.; Keskin, D. B. A large peptidome dataset improves HLA class I epitope prediction across most of the human population. *Nat. Biotechnol.* **2020**, *38* (2), 199−209.

(30) Vita, R.; Zarebski, L.; Greenbaum, J. A.; Emami, H.; Hoof, I.; Salimi, N.; Damle, R.; Sette, A.; Peters, B. The immune epitope database 2.0. *Nucleic Acids Res.* **2010**, *38* (Database issue), D854−D862.

(31) Nguyen, A.; David, J. K.; Maden, S. K.; Wood, M. A.; Weeder, B. R.; Nellore, A.; Thompson, R. F. Human leukocyte antigen susceptibility map for SARS-CoV-2. *J. Virol.* **2020**, DOI: 10.1128/JVI.00510-20.

(32) Reynisson, B.; Alvarez, B.; Paul, S.; Peters, B.; Nielsen, M. NetMHCpan-4.1 and NetMHCIIpan-4.0: improved predictions of MHC antigen presentation by concurrent motif deconvolution and integration of MS MHC eluted ligand data. *Nucleic Acids Res.* **2020**, *48* (W1), W449−W454.

(33) Komov, L.; Kadosh, D. M.; Barnea, E.; Milner, E.; Hendler, A.; Admon, A. Cell Surface MHC Class I Expression Is Limited by the Availability of Peptide-Receptive "Empty" Molecules Rather than by

https://dx.doi.org/10.1021/acs.jproteome.0c00457
J. Proteome Res. XXXX, XXX, XXX−XXX

the Supply of Peptide Ligands. *Proteomics* **2018**, *18* (12), No. e1700248.
(34) Hearn, A.; York, I. A.; Rock, K. L. The specificity of trimming of MHC class I-presented peptides in the endoplasmic reticulum. *J. Immunol.* **2009**, *183* (9), 5526−36.
(35) Georgiadou, D.; Hearn, A.; Evnouchidou, I.; Chroni, A.; Leondiadis, L.; York, I. A.; Rock, K. L.; Stratikos, E. Placental leucine aminopeptidase efficiently generates mature antigenic peptides in vitro but in patterns distinct from endoplasmic reticulum aminopeptidase 1. *J. Immunol.* **2010**, *185* (3), 1584−92.
(36) Kuiper, J. J.; Van Setten, J.; Ripke, S.; Van, T. S. R.; Mulder, F.; Missotten, T.; Baarsma, G. S.; Francioli, L. C.; Pulit, S. L.; De Kovel, C. G.; Ten Dam-Van Loon, N.; Den Hollander, A. I.; Huis in het Veld, P.; Hoyng, C. B.; Cordero-Coma, M.; Martin, J.; Llorenc, V.; Arya, B.; Thomas, D.; Bakker, S. C.; Ophoff, R. A.; Rothova, A.; De Bakker, P. I.; Mutis, T.; Koeleman, B. P. A genome-wide association study identifies a functional ERAP2 haplotype associated with birdshot chorioretinopathy. *Hum. Mol. Genet.* **2014**, *23* (22), 6081−6087.
(37) Grifoni, A.; Weiskopf, D.; Ramirez, S. I.; Mateus, J.; Dan, J. M.; Moderbacher, C. R.; Rawlings, S. A.; Sutherland, A.; Premkumar, L.; Jadi, R. S.; Marrama, D.; de Silva, A. M.; Frazier, A.; Carlin, A. F.; Greenbaum, J. A.; Peters, B.; Krammer, F.; Smith, D. M.; Crotty, S.; Sette, A. Targets of T Cell Responses to SARS-CoV-2 Coronavirus in Humans with COVID-19 Disease and Unexposed Individuals. *Cell* **2020**, *181* (7), 1489−1501.
(38) Wilk, A. J.; Rustagi, A.; Zhao, N. Q.; Roque, J.; Martinez-Colon, G. J.; McKechnie, J. L.; Ivison, G. T.; Ranganath, T.; Vergara, R.; Hollis, T.; Simpson, L. J.; Grant, P.; Subramanian, A.; Rogers, A. J.; Blish, C. A. A single-cell atlas of the peripheral immune response in patients with severe COVID-19. *Nat. Med.* **2020**, *26* (7), 1070−1076.
(39) Wang, W.; Zhang, W.; Zhang, J.; He, J.; Zhu, F. Distribution of HLA allele frequencies in 82 Chinese individuals with coronavirus disease-2019 (COVID-19). *HLA* **2020**, *96* (2), 194−196.
(40) de Castro, J. A. L. How ERAP1 and ERAP2 Shape the Peptidomes of Disease-Associated MHC-I Proteins. *Front. Immunol.* **2018**, *9*, 2463.
(41) Infantes, S.; Samino, Y.; Lorente, E.; Jimenez, M.; Garcia, R.; Del Val, M.; Lopez, D. Cutting Edge: H-2L(d) Class I Molecule Protects an HIV N-Extended Epitope from In Vitro Trimming by Endoplasmic Reticulum Aminopeptidase Associated with Antigen Processing. *J. Immunol.* **2010**, *184* (7), 3351−3355.
(42) Thomas, C.; Tampe, R. MHC I chaperone complexes shaping immunity. *Curr. Opin. Immunol.* **2019**, *58*, 9−15.
(43) Chen, H.; Li, L.; Weimershaus, M.; Evnouchidou, I.; van Endert, P.; Bouvier, M. ERAP1-ERAP2 dimers trim MHC I-bound precursor peptides; implications for understanding peptide editing. *Sci. Rep.* **2016**, *6*, 28902.
(44) Mavridis, G.; Arya, R.; Domnick, A.; Zoidakis, J.; Makridakis, M.; Vlahou, A.; Mpakali, A.; Lelis, A.; Georgiadis, D.; Tampe, R.; Papakyriakou, A.; Stern, L. J.; Stratikos, E. A systematic re-examination of processing of MHCI-bound antigenic peptide precursors by endoplasmic reticulum aminopeptidase 1. *J. Biol. Chem.* **2020**, *295* (21), 7193−7210.
(45) Perez-Riverol, Y.; Csordas, A.; Bai, J.; Bernal-Llinares, M.; Hewapathirana, S.; Kundu, D. J.; Inuganti, A.; Griss, J.; Mayer, G.; Eisenacher, M.; Perez, E.; Uszkoreit, J.; Pfeuffer, J.; Sachsenberg, T.; Yilmaz, S.; Tiwary, S.; Cox, J.; Audain, E.; Walzer, M.; Jarnuczak, A. F.; Ternent, T.; Brazma, A.; Vizcaino, J. A. The PRIDE database and related tools and resources in 2019: improving support for quantification data. *Nucleic Acids Res.* **2019**, *47* (D1), D442−D450.

https://dx.doi.org/10.1021/acs.jproteome.0c00457
J. Proteome Res. XXXX, XXX, XXX−XXX